LBL-29714
Preprint

Center for Advanced Materials

CAM

Submitted to the Journal of Vacuum Science and Technology

Tip-Surface Forces During Imaging by Scanning Tunneling Microscopy

M. Salmeron, D.F. Ogletree, C. Ocal, H.-C. Wang,
G. Neubauer, and W. Kolbe

October 1990

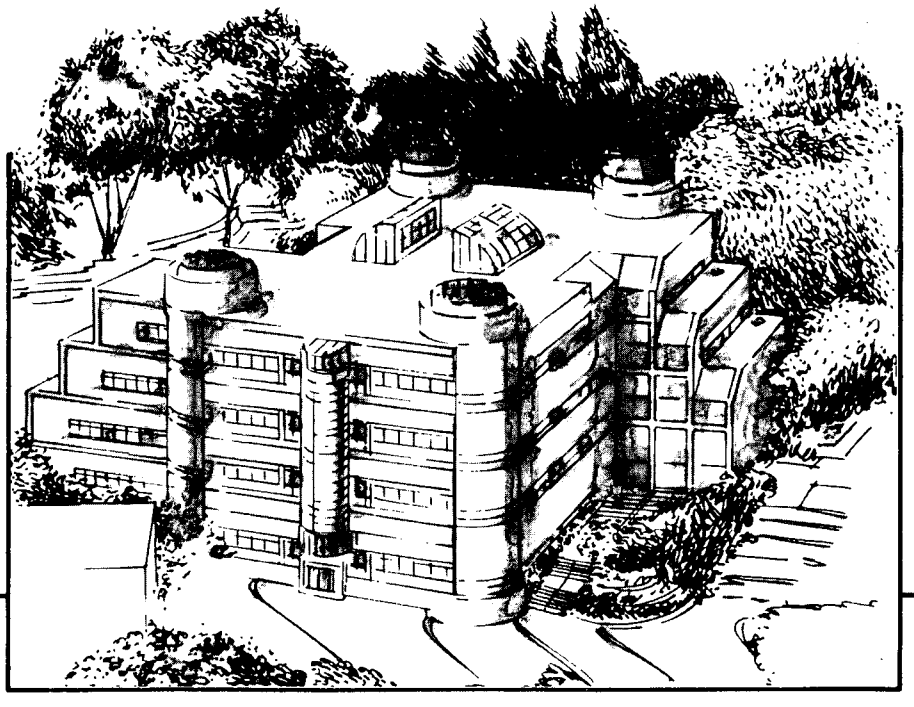

Materials and Chemical Sciences Division

Lawrence Berkeley Laboratory • University of California

ONE CYCLOTRON ROAD, BERKELEY, CA 94720 • (415) 486-4755

Prepared for the U.S. Department of Energy under Contract DE-AC03-76SF00098

LOAN COPY
Circulates
for 2 weeks
LBL-29714
Copy 2
Bldg. 50 Library.

DISCLAIMER

This document was prepared as an account of work sponsored by the United States Government. While this document is believed to contain correct information, neither the United States Government nor any agency thereof, nor the Regents of the University of California, nor any of their employees, makes any warranty, express or implied, or assumes any legal responsibility for the accuracy, completeness, or usefulness of any information, apparatus, product, or process disclosed, or represents that its use would not infringe privately owned rights. Reference herein to any specific commercial product, process, or service by its trade name, trademark, manufacturer, or otherwise, does not necessarily constitute or imply its endorsement, recommendation, or favoring by the United States Government or any agency thereof, or the Regents of the University of California. The views and opinions of authors expressed herein do not necessarily state or reflect those of the United States Government or any agency thereof or the Regents of the University of California.

LBL-29714

TIP-SURFACE FORCES DURING IMAGING BY SCANNING TUNNELING MICROSCOPY

M. Salmeron, D.F. Ogletree, C. Ocal[1]
H.-C. Wang, G. Neubauer and W. Kolbe[2]

Materials Science Division
Center for Advanced Materials
and [2]Engineering Division
Lawrence Berkeley Laboratory
University of California
Berkeley, CA 94720 U.S.A.

G. Meyers

DOW Chemical Company, Midland, MI

[1]Departamento de Materia Condensada, Universidad Utonoma de Madrid, Madrid, Spain

ACKNOWLEDGMENT
This work was supported by Exploratory Funds from the Director, Office of Energy Research, Office of Basic Energy Sciences, Material Sciences Division, U.S. Department of Energy under contract No. DE-AC03--76SF00098.

TIP-SURFACE FORCES DURING IMAGING BY SCANNING TUNNELING MICROSCOPY

M. Salmeron, D.F. Ogletree, C. Ocal[1]
H.-C. Wang, G. Neubauer and W. Kolbe[2]

Materials and Chemical Science Division
and [2]Engineering Division
Lawrence Berkeley Laboratory
1 Cyclotron Road
Berkeley, CA 94720 USA

G. Meyers

DOW Chemical Company, Midland, MI

ABSTRACT

The effect of compressive and shear forces between tip and surface during the operation of the Scanning Tunneling Microscope is illustrated with examples obtained both in air and vacuum environments. We show that at typical gap resistances used in STM ($\leq$ 20 GΩ) these forces can have significant effects. Compressive or repulsive forces give rise to anomalous topographic corrugations (elastic deformations) as well as to permanent damage (inelastic or plastic deformation). These forces also cause the anomalously low values obtained in measurements of the tunneling barrier height. The effects of shear forces when imaging weakly bound material will also be demonstrated.

1. INTRODUCTION

The existence of forces between the tip and the surface in the Scanning Tunneling Microscope has been recognized since the invention of the instrument.[1] The measurement and control of these forces led to the development of a new instrument, the Atomic Force Microscope.[2] Due to tip-surface forces, there can be gross distortions in STM images and damage to the surface in the extreme of large forces (plastic deformation), and more subtle effects that affect image interpretation when the forces are smaller and their action reversible (elastic region). The anomalous atomic corrugation observed in graphite[3,4] is one of the best known examples of the effects of compressive forces. Mamin *et al.* have linked the abnormally high corrugations on graphite to a contamination-mediated deformation of the graphite surface. They have shown that corrugations of < 1Å and current *vs.* distance curves steeper by two orders of magnitude than in air can only be obtained by cleaning tip and sample in UHV.[5]

[1]Departamento de Materia Condensada, Universidad Autonoma de Madrid, Madrid, Spain

The purpose of this paper is to illustrate for various samples, which differ in their bulk properties (elastic moduli) as well as their intermolecular (chemical) interaction with the tip, the effect of the short-range repulsive part of the tip-surface forces on STM images. We will present data in air as well as UHV environment and will link the operation of these forces with the measurement of very low work function values. Finally, we will illustrate that the shear or frictional component of the tip-surface force also becomes important when tip and sample are in contact.

2. EXPERIMENTAL

The experimental results presented in this paper were obtained using a variety of STM instruments in two laboratories operating in different environments. The STM's used a single piezo tube for xyz tip motion. Tip-sample approaches were performed by means of fine screws or by inertial displacement using an auxiliary piezo tube concentric to the scanner.[6] Most of the results presented here were obtained in air, particularly those decribed in section 3 and when using graphite. The results on sulfur overlayers were obtained in high vacuum (10^{-7} torr) and in UHV (10^{-10} torr). An atomic force microscope (AFM) of the interferometric type, similar to that described by Erlandsson *et al.*, was used to measure forces during graphite STM imaging.[7]

3. IMAGING UNDER STRONG COMPRESSIVE FORCES: THE PLASTIC REGIME

We start by illustrating the effect of oxide layers on tungsten tips, a common situation during operation in air. A layer of oxide might become apparent by instability in the gap width as the feedback loop tries to maintain a constant value of the tunneling current. We would like to point out that in this context the gap represents the distance between the delocalized electronic states in the tip and surface between which electron transfer occurs. The insulating oxide layer is then part of the gap.The thicker the oxide layer and the smaller the gap resistance (i.e., ratio of applied bias voltage and measured current), which decreases with gap width, the more likely mechanical contact of tip and sample is to occur. That will result in compression of the gap and eventually damage of tip or sample when the elastic response limit of the materials involved is exceeded.

Figure 1 represents an example of such behavior: A nickel CD stamper is imaged with a tungsten tip operating at a gap resistance of 68MΩ in air (fig. 1a). After scanning for 15 minutes, severe erosion has been caused by the tip force, as indicated by the debris accumulated in the trough regions. Since substantial plastic deformation has obviously occurred, the pressure during scanning probably exceeded 210 GPa or $2.1 \times 10^{11} N/m^2$, if we take the elastic modulus of Ni. When the gap resistance is increased to 38GΩ, no visible damage occurs, as shown in fig. 1b. We assume that in this case tip and surface are not in contact any more. In a control experiment with a less reactive PtIr tip, which should not form a bulk oxide layer, no damage was found when imaging at the reduced gap of 62 MΩ.

4. IMAGING UNDER WEAK COMPRESSIVE FORCES: THE ELASTIC REGIME

The onset of plastic behavior depends not only on the elastic threshold as a specific material bulk property, but also on the strength of intermolecular (chemical) interactions between tip and sample. Two clean metal surfaces, for example, will exhibit a transition from elastic to plastic behavior over a small range of applied forces, with plastic deformation sometimes found at zero applied force as a consequence of forces of adhesion.[17] Alternately, in the absence of strong (chemical) interaction between tip and sample, stable and reproducible images can be produced, as long as the compressive forces, which might be present, do not exceed the elastic limits of tip or sample. There are two typical signatures of this case of imaging. One is the observation of anomalously large atomic corrugations, often several times the expected electronic corrugation. The other is the measurement of very low values of the barrier height. Graphite provides the most widely known example of giant corrugations,[3] but other materials can show similar effects when the STM is operated in air or in UHV, as we will show in the next section.

Once the tip-surface gap is being compressed, forces are acting on the entire mechanical loop linking tip and sample, and most of the displacement will be absorbed by deformation of the weakest part in the loop. Again, as a reminder, when the gap is defined as the distance between the electronic states where electron transfer occurs, any non-conducting adsorption or

contamination layer is included in the gap. The schematic drawing in figure 2 illustrates the concept. Here $k_{gap}, k_{surface}$ and k_{tip} are the spring constants of the gap, the sample being imaged and the STM, respectively, Δz_{surf} and Δz_{tip} are deformations of surface and tip, respectively. The true change in gap distance Δz_{gap}, i.e., the true surface corrugation, is related to the z-piezo displacement Δz_{piezo} by:

$$\Delta z_{piezo} = \Delta z_{gap} + \Delta z_{surface} + \Delta z_{tip}$$

$$\Delta z_{gap} = (1 + k_{gap}\frac{k_{surface} + k_{tip}}{k_{surface}k_{tip}})^{-1}\Delta z_{piezo} = \alpha^{-1}\Delta z_{piezo}$$

When $\alpha > 1$ the measured or apparent corrugation Δz_{piezo} will be larger than the true change in the gap.

4.1 Forces acting during tunneling when imaging graphite

The effects of tip and surface deformation can be easily demonstrated in a combined AFM/ STM instrument where the tip cantilever is designed to be the weakest mechanical link. We simultaneously measured normal lever deflection and current while bringing the sample repeatedly up to and beyond the point of hard contact, where the lever starts bending backwards due to the pressure of the advancing sample. Current in these experiments was detected just at the onset of repulsive force and, depending on the sharpness of the tip, generally required repulsive forces in the 10^{-6} N range to reach currents of a few nA. Similar results have been found by others.[8]

We then acquired a topographic STM image of graphite under such repulsive force at a current of 8nA and a bias of 50mV while simultaneously recording the AFM lever deflection. Similar experiments have also been performed by others.[8] Figure 3 reflects the remarkable agreement between the cantilever deflection (fig. 3b) and the corresponding STM piezo displacement topographic image (fig. 3a). From the calibrated line scans in figure 4 we obtain an average topographic corrugation of $\sim$ 9Å while the average lever deflection corrugation is $\sim$ 6Å, corresponding to a force corrugation of 2×10^{-7} N (cantilever $k = 310$ N/m). From the average lever deflection of 28Å during these measurements we derive an average load of $\sim 9 \times 10^{-7}$ N during imaging. The difference between the two corrugations suggests that another component in the mechanical loop, presumably the graphite sample, is deforming with an effective spring constant of $\sim$ 600 N/m.

Using the elastic modulus of graphite[5], such a spring constant can be obtained for a small flake, which might have attached to the tip, of size 200Å × 200Å and thickness 130 Å (see also section 4.4).

4.2 Elastic properties of sulfur monolayers on metals

We conducted a series of experiments to measure the changes in tunnel current as a function of tip displacement on a sulfur covered Re(0001) surface. An ordered $(2\sqrt{3} \times 2\sqrt{3})R30^0$ sulfur overlayer was prepared in UHV and the sample was transferred through air to an STM operating in a 10^{-7} Torr vacuum.[10] We have demonstrated earlier by LEED, Auger, and STM that a saturation coverage of sulfur (0.5 monolayer) prevents oxidation of the Re(0001) surface when exposed to air.[9,10,11] STM images showed corrugations due to sulfur atoms between 0.2 and 4 Å depending on the tip shape. For comparison, LEED calculations on other structures indicate that sulfur adatoms are typically located $\sim$ 1.3 Å above the top layer metal atoms.

In the experiments presented here, the $(2\sqrt{3} \times 2\sqrt{3})R30^0$ sulfur structure was first imaged in the topographic mode at a gap resistance of 20 MΩ and a -16mV sample bias. The tip was then positioned in the middle of the image, the feedback loop was disabled, and the tip was advanced until a predetermined current I_{max} was obtained. Currents as large as 900 nA were obtained after z piezo displacements of 20 Å, as shown in figure 5. The gap resistance reached values as low as 20 kΩ, on the order of the Sharvin point contact resistance.[18] However, no changes were seen in atomic resolution images of the sulfur overlayer recorded before and after tip approach, indicating that only elastic deformations of the tip or sample took place.

Tip-surface forces could not be directly measured in these STM experiments. However, if we assume that most of the 20 Å displacement is due to elastic deformations of tip or sample, we can get to an estimate: First, we assume a rigid gap and a deformable tip and/or surface with increasing area of contact as the tip advances. The increase in current would then be proportional to the increase in contact area and we can treat the measured gap resistance as the Sharvin resistance $R = 4\rho l/3\pi a^2$.[18] Here ρ is the specific resistivity of the material, l is the

electron mean free path, and $a = a(z)$ is the radius of the circular contact area which depends on the tip shape as the only parameter: Indeed, we obtain a good fit to the data of figure 5 by implying a conical tip (solid line). Using the elastic moduli of Re and PtRh, and a radius of 100 Å for the tip (estimated from the observed step widths) the initial compressive force is estimated to be of the order of 10^{-6} N and the maximum gap pressure $\sim$ 10 GPa.

4.3 The origin of low work function values in STM

Unrealistically small values of ϕ, the work function (or more accurately, the local barrier height), measured in $I - z$ or $\partial I/\partial z$ experiments indicate the presence of tip-surface forces. For the system described in the last section, for example, we find $\phi = 90$ meV from the initial slope of the $I - z$ curve in figure 5, if $\Delta z_{gap} = \Delta z_{piezo}$.

We also made a series of $\partial I/\partial z$ measurements at different gap resistances for a PtRh tip and a clean Rh(111) substrate in UHV. The barrier height $\phi = (\partial I/I_0 \partial z)^2$ is plotted as a function of gap resistance in figure 6. As we can see "normal" values of ϕ (above a few eV's) independent of R_{gap} were not obtained until R_{gap} exceeded 20 GΩ. Since we obtained stable images and did not observe any damage at gaps as small as 20MΩ for clean Rh, we believe that the expected strong adhesion of clean metal surfaces,[17] (which can cause surface damage even at applied forces well below the elastic threshold - see section 4), is prevented due to a passivating contamination layer such as carbon on the tip.

Elastic tip and sample deformations are not the only source of low ϕ values. Lang has demonstrated through model calculations that the tunnel barrier collapses for tip-sample gaps of a few Å.[13] The results of Lang's calculations were expressed in terms of gap resistance and replotted in figure 6 (dashed line) for comparison with our experiment: The experimental results have a different functional form and drop off much more quickly than predicted by Lang's theory. This comparison is not intended as a test of Lang's results, but rather to show that the electronic effect of barrier collapse alone is not sufficient to explain the magnitude of the decrease in ϕ and that in the presence of strong repulsive forces the elastic deformation mechanism has a substantial effect.

4.4 Shear forces during STM imaging

The presence of shear or frictional force components parallel to the surface is to be expected in view of the above observations: the surface damage described above, is certainly the result of both force components since lateral displacement of debris is observed. These forces have been measured directly only by McClelland and collaborators.[7,14,15]

As with compressive forces, frictional forces can cause elastic and inelastic effects: As evidence for elastic effects of frictional forces, we found in STM images of graphite, recorded with a long tapered etched tip (from electron micrographs), significant distortions of the lattice and featureless regions over several Å at the start of each scanning line. Others have reported similar results.[16]

Two dimensional graphite flakes provide another dramatic demonstration of shear forces during STM imaging, in this particular example for their inelastic effects: One small flake $\sim$ 200 Å in diameter was observed in several large scale topographic images. The flake appeared to shift in position from one image to another. The tip was then positioned on top of the flake and a 20 Å square topographic image was acquired (figure 7). A highly distorted graphite unit cell was imaged with dimensions of 4 and 7 Å in the x and y directions, respectively, 2 to 3 times larger than the undistorted cell. We believe that the tip is dragging the flake back and forth, with different effects in the x (fast raster) and y (slow raster) directions.

5. SUMMARY

We have shown that, under rather typical tunneling conditions, significant repulsive forces acting in the compression and in the shear modes are more the rule than the exception: Both plastic and elastic effects can occur depending on the intermolecular interaction of tip and sample and the force, or better pressure, as compared to the elastic threshold as a bulk property. When operating below the elastic thresholds of the materials involved and in the absence of a strong chemical interaction between tip and sample, the deformations can be elastic and reversible. They manifest themselves through the anomalous corrugation values obtained for many surface structures, and also in the very low values of the work function obtained in STM experiments.

Acknowledgments

The graphite flake image in figure 7 was acquired by T.P. Beebe and J. Odriozola. This work has been supported by Exploratory Funds from the Director, Office of Energy Research, Basic Energy Science, Materials Division of the US Department of Energy under contract number DE-AC03-76SF00098. Additional support has been provided by a grant from the DOW Chemical Company.

REFERENCES

1. G. Binnig, H. Rohrer, Ch. Gerber, and E. Weibel, Phys. Rev. Lett. **49**, 57,1982.
2. G. Binnig, C. F. Quate, and Ch. Gerber, Phys. Rev. Lett. **56**, 930, 1986.
3. J. M. Soler, A. M. Baró, N. Garcia, and H. Rohrer, Phys. Rev. Lett. **57**, 444 (1986).
4. J. H. Coombs and J. B. Pethica, IBM J. Res. Develop. **30**, 455 (1986).
5. H. J. Mamin, E. Ganz, D. W. Abraham, R. E. Thomson, and J. Clarke, Phys. Rev. **B 34**, 9015 (1986).
6. D. M. Zeglinski, D. F. Ogletree, R. Q. Hwang, T. P. Beebe, G. A. Somorjai, and M. B. Salmeron, Rev. Sci. Instr., in press (1990).
7. R. Erlandsson, G. Hadziioannou, C. M. Mate, G. M. McClelland, and S. Chiang, J. Vac. Sci. Technol. A **6**, 266 (1988).
8. C. M. Mate, R. Erlandsson, G. M. McClelland, and S. Chiang, Surf. Sci. **208**, 473 (1988).
9. B. Marchon, P. Bernhardt, M. E. Bussell, G. A. Somorjai, M. Salmeron, and W. Siekhaus, Phys. Rev. Lett. **60**, 1166, (1988).
10. D. F. Ogletree, C. Ocal, B. Marchon, M. B. Salmeron, G. A. Somorjai, T. P. Beebe, and W. Siekhaus, J. Vac. Sci. Technol. A **8**, 297 (1990).
11. D. G. Kelly, A. J. Gellman, M. Salmeron, G. A. Somorjai, V. Maurice, M. Huber, and J. Oudar, Surf. Sci. **204**, 1 (1988).

12. R. Q. Hwang, D. M. Zeglinski, D. F. Ogletree, G. A. Somorjai, and M. B. Salmeron, J. Vac. Sci. Technol. A **9**, STM V proceedings (1991).

13. N. D. Lang, Phys. Rev. B **37**, 10395 (1988).

14. C. M. Mate, G. M. McClelland, R. Erlandsson, and S. Chiang, Phys. Rev. Lett. **59**, 1942 (1987).

15. G. Neubauer, S. R. Cohen, G. M. McClelland, D. Horne, and C. M. Mate, Rev. Sci. Instr., **61**, in press (1990).

16. S. L. Tang, J. Bokor, and B. H. Storz, Appl. Phys. Lett. **52**, 188 (1988).

17. Q. Guo, J. D. J. Ross, and H. M. Pollock, in: New Materials Approaches to Tribology: Theory and Application, edited by L. E. Pope, L. Fehrenbacher, and W. O. Winter (Mater. Res. Soc., Pittsburgh, 1989), **140**, 51 (1989).

18. A. G. M. Jansen, A. P. van Gelder, and P. Wyder, J. Phys. C, Solid St. Phys., **13**, 6073 (1980).

FIGURE CAPTIONS

Figure 1: Images of a nickel compact disk (CD) stamper showing top view grey scale images and cross sections.
(a) A $6 \times 6\mu$m image recorded with a tungsten tip at $R_{gap} = 68$ MΩ, and the same image after scanning the central $2 \times 2\mu$m part of the image for 15 minutes. Substantial surface damage can be seen: At this gap resistance the gap distance is thus less than the oxide layer thickness.
(b) A $6 \times 6\mu$m image of a new area recorded with a tungsten tip at $R_{gap} = 28$ GΩ, and the same image after scanning the central $2 \times 2\mu$m part of the image for 20 minutes. There is no apparent change in the surface structure: the gap distance now is larger than the oxide thickness.

Figure 2: Schematic drawing showing the effect of the tip and sample compliance on the tunnel gap. Deformations of the tip and surface make the change in the tunnel gap Δz_{gap} less than the applied displacement Δz_{piezo}.

Figure 3: Forces during STM imaging of a graphite surface with a PtRh tip: (a) Topographic image of an HOPG sample (vertical scale arbitrary units) recorded at 8nA and 50 mV; (b) Simultaneously recorded cantilever deflection showing the forces acting on the tip during tunneling. Note the perfect registry of the two images. Horizontal streaks are due to unfiltered low frequency noise.

Figure 4: Forces during STM imaging of a graphite surface with a PtRh tip. Calibrated line profile over 15 Å in the sample x direction showing several periods of the graphite lattice. The cantilever displacement and the z piezo displacement were measured simultaneously.

Figure 5: Tunnel current and gap resistance as a function of tip displacement for a Re(0001) surface with a $(2\sqrt{3} \times 2\sqrt{3})$R30^0 sulfur overlayer and a PtRh tip. Tip displacement is measured relative to the initial tunneling conditions of 8 nA and -16mV sample bias. The symbols show different runs from the same sample and tip and the solid line is calculated by assuming the current increase is due solely to an increase of the area of contact for a conical tip.

Figure 6: The solid line shows the experimental decrease inϕ as a function of R_{gap} for a PtRh tip and a clean Rh(111) surface in UHV. The dashed line shows the results of Lang's $\phi(z)$ calculations on a different system replotted in terms of R_{gap} for comparison.

Figure 7: An 18 Å square topographic image (-100mV sample bias, 100 MΩ gap resistance) acquired on top of a two dimensional $\sim$ 200 Å graphite flake. The tip is dragging the flake back and forth, grossly distorting the image.

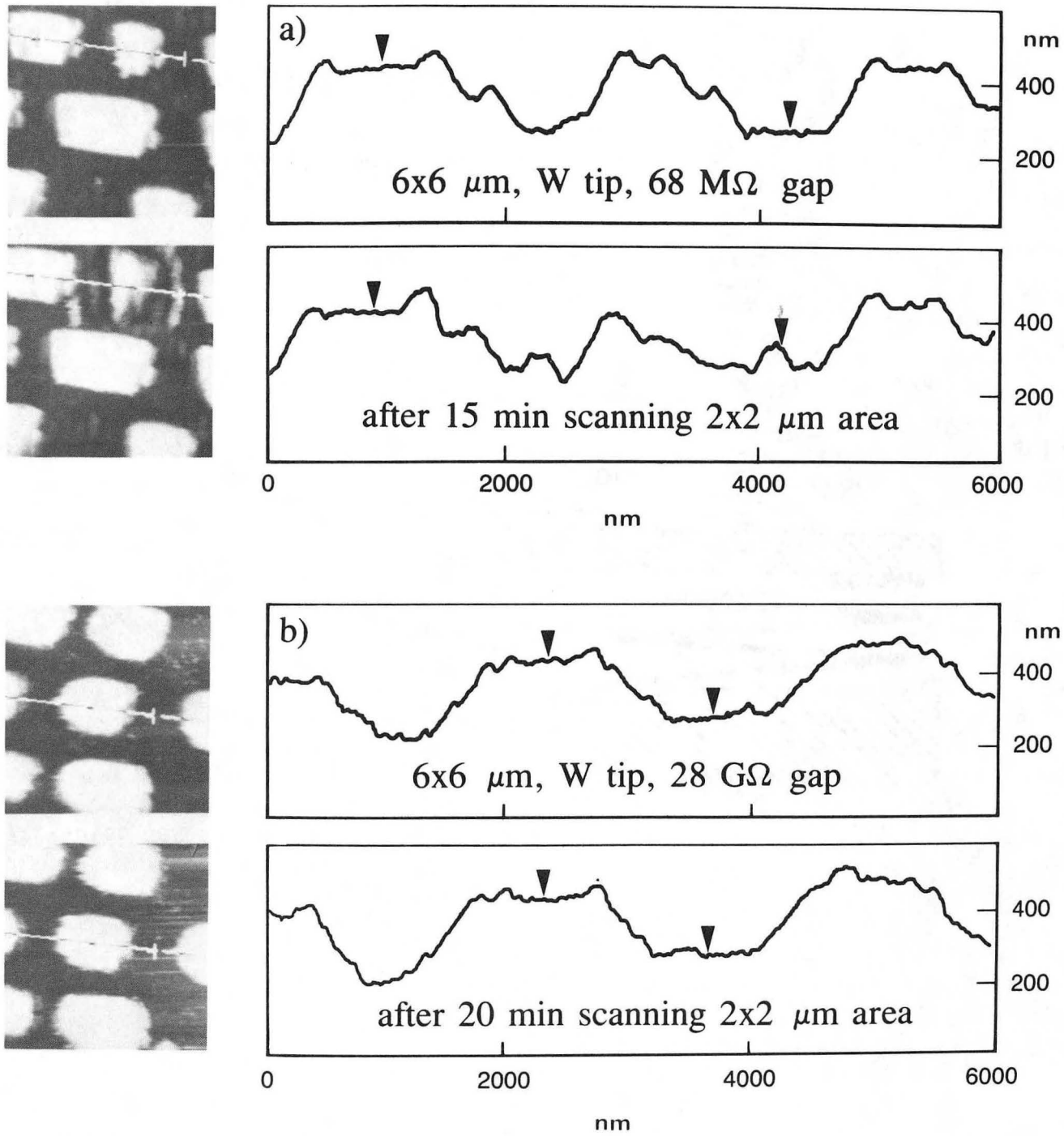

XBB900-8310

Figure 1

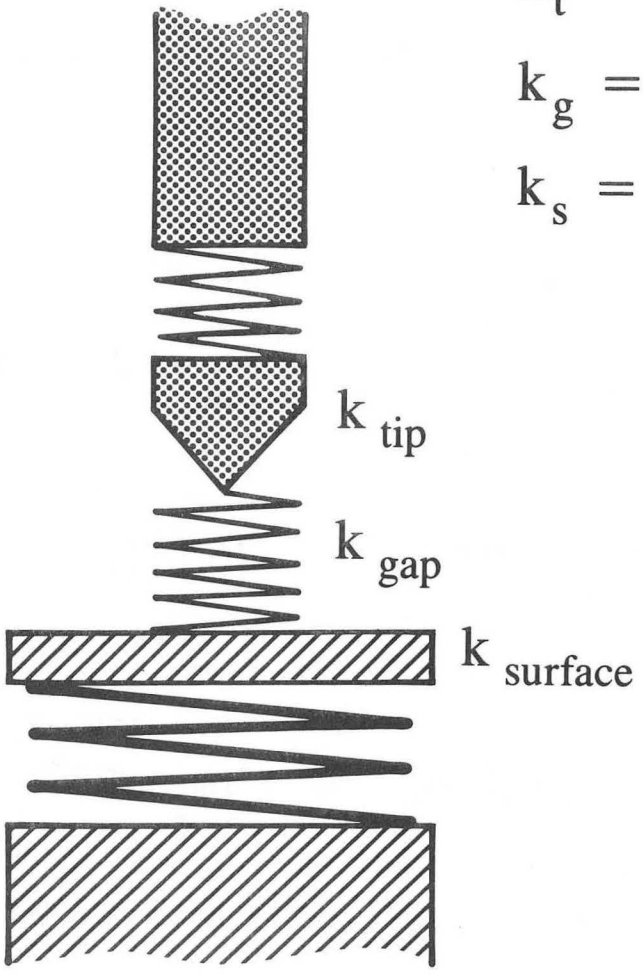

k_t = tip force constant

k_g = gap force constant

k_s = surface force constant

XBL 9010-3324

Figure 2

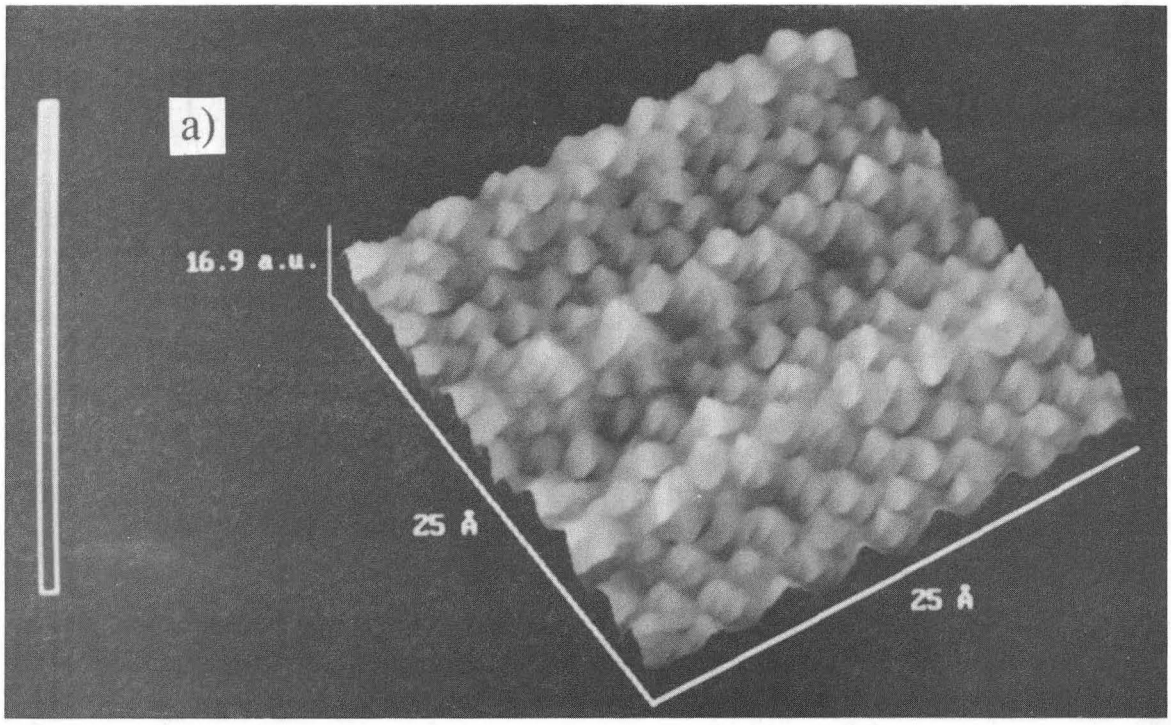

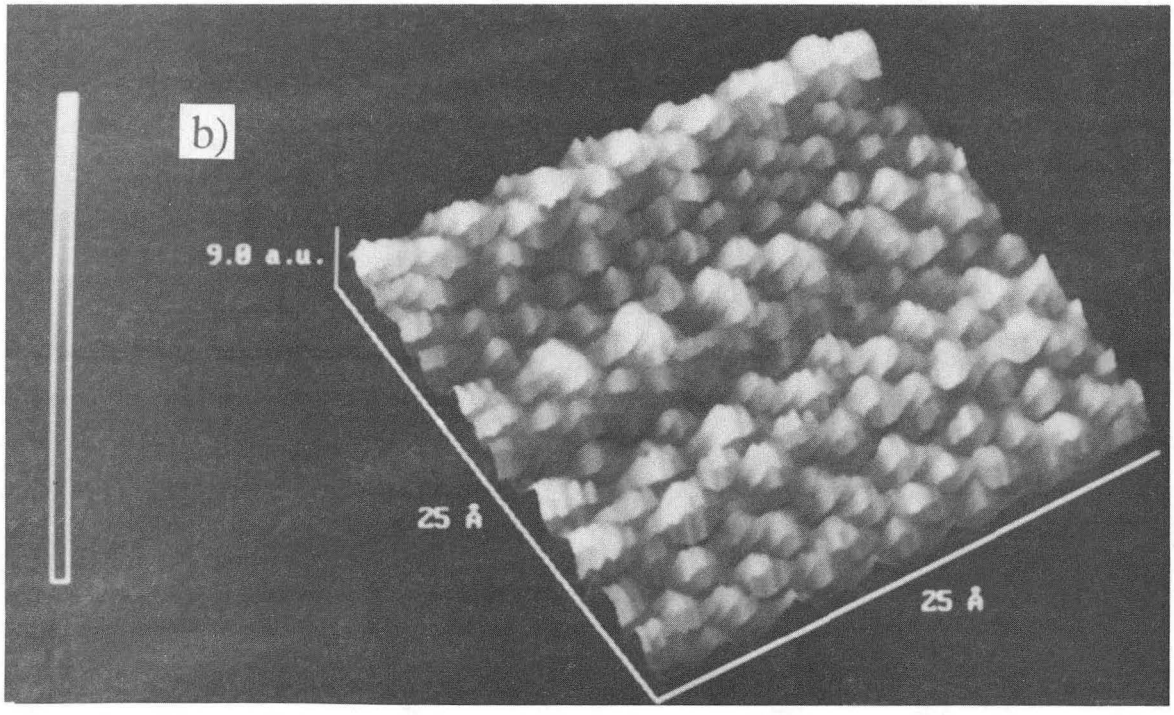

CBB 907-5645

Figure 3

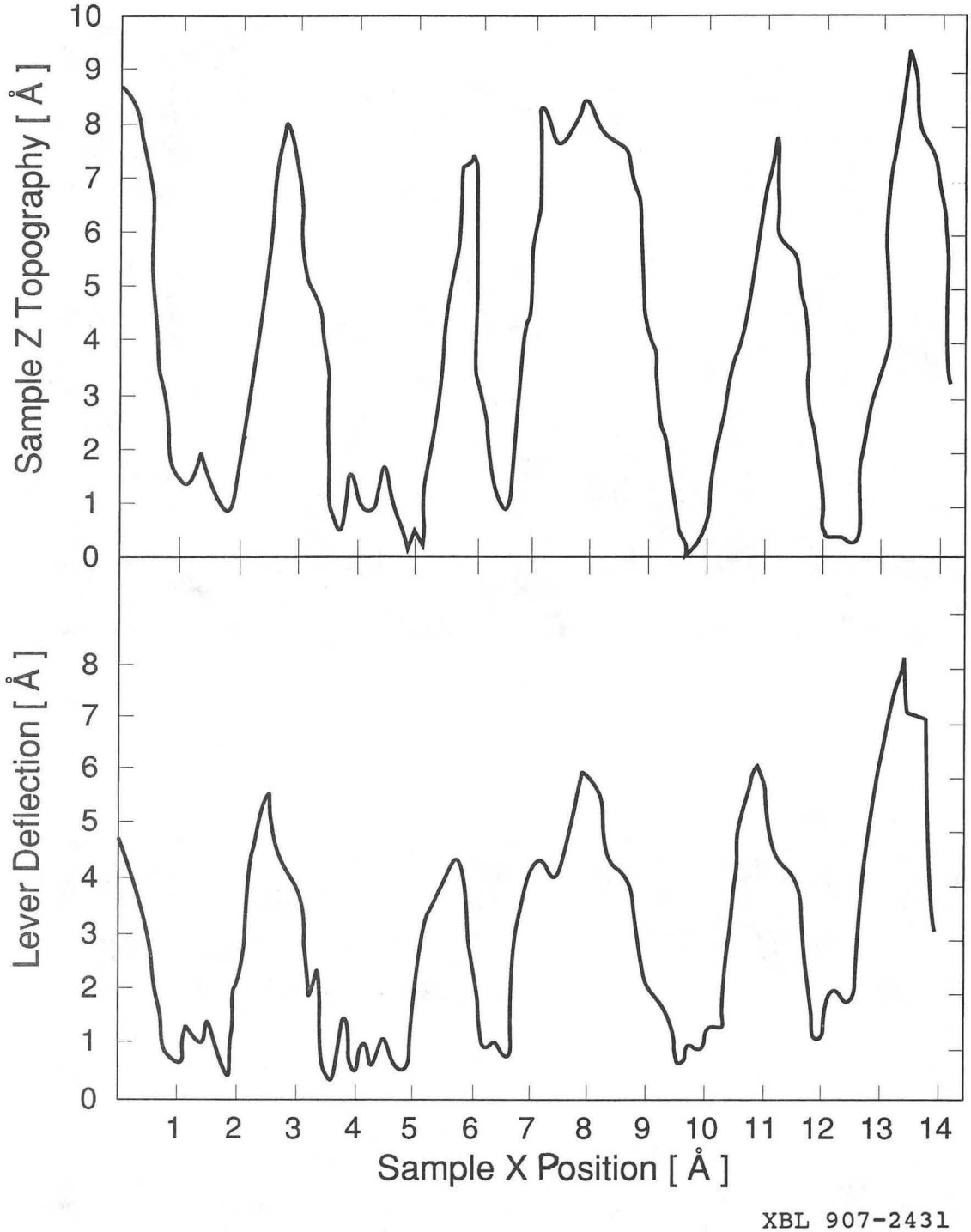
Sample Z Topography [Å]
Lever Deflection [Å]
Sample X Position [Å]
0
1
2
3
4
5
6
7
8
9
10
11
12
13
14
XBL 907-2431

Figure 4

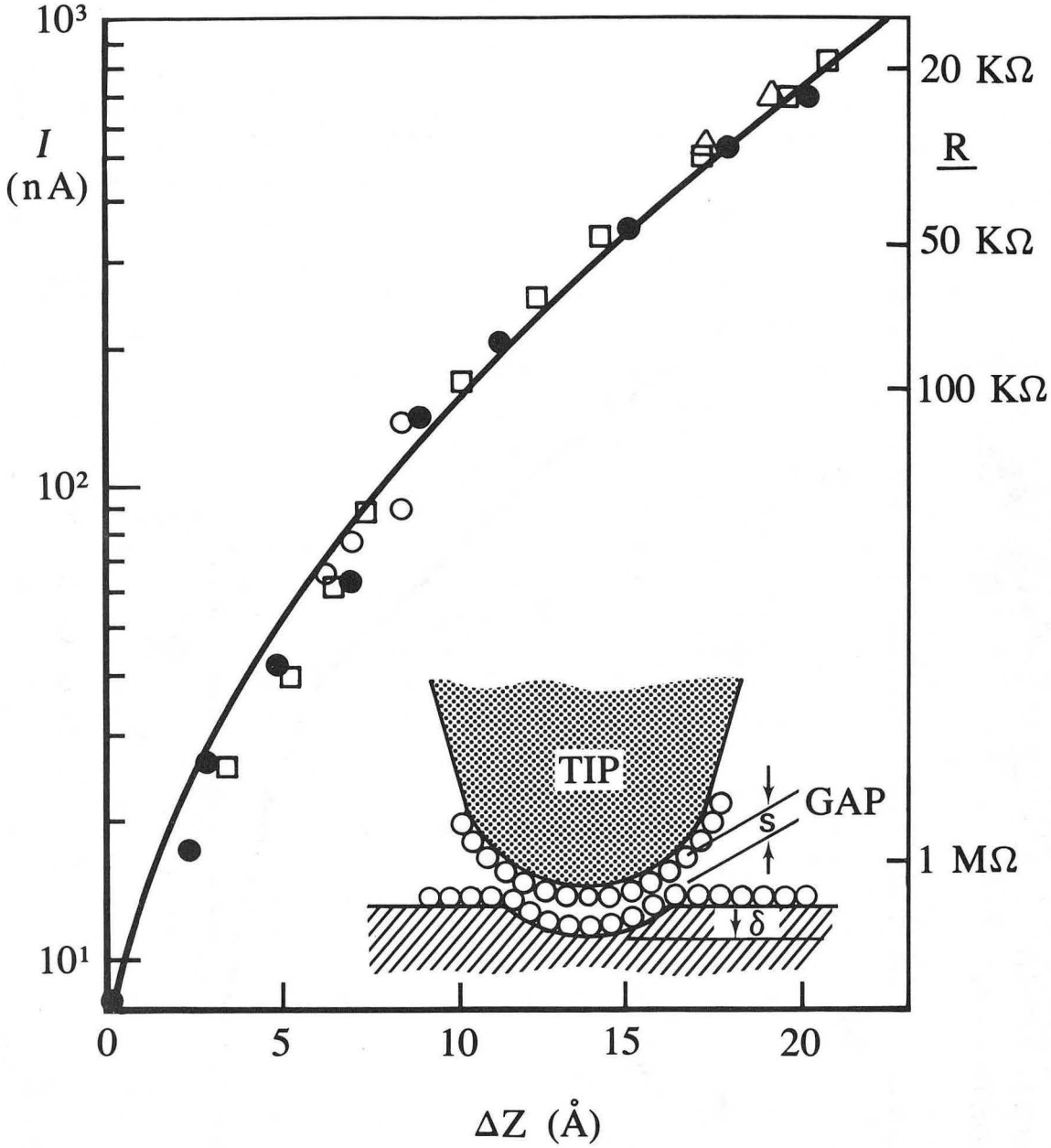

XBL 9010-3325

Figure 5

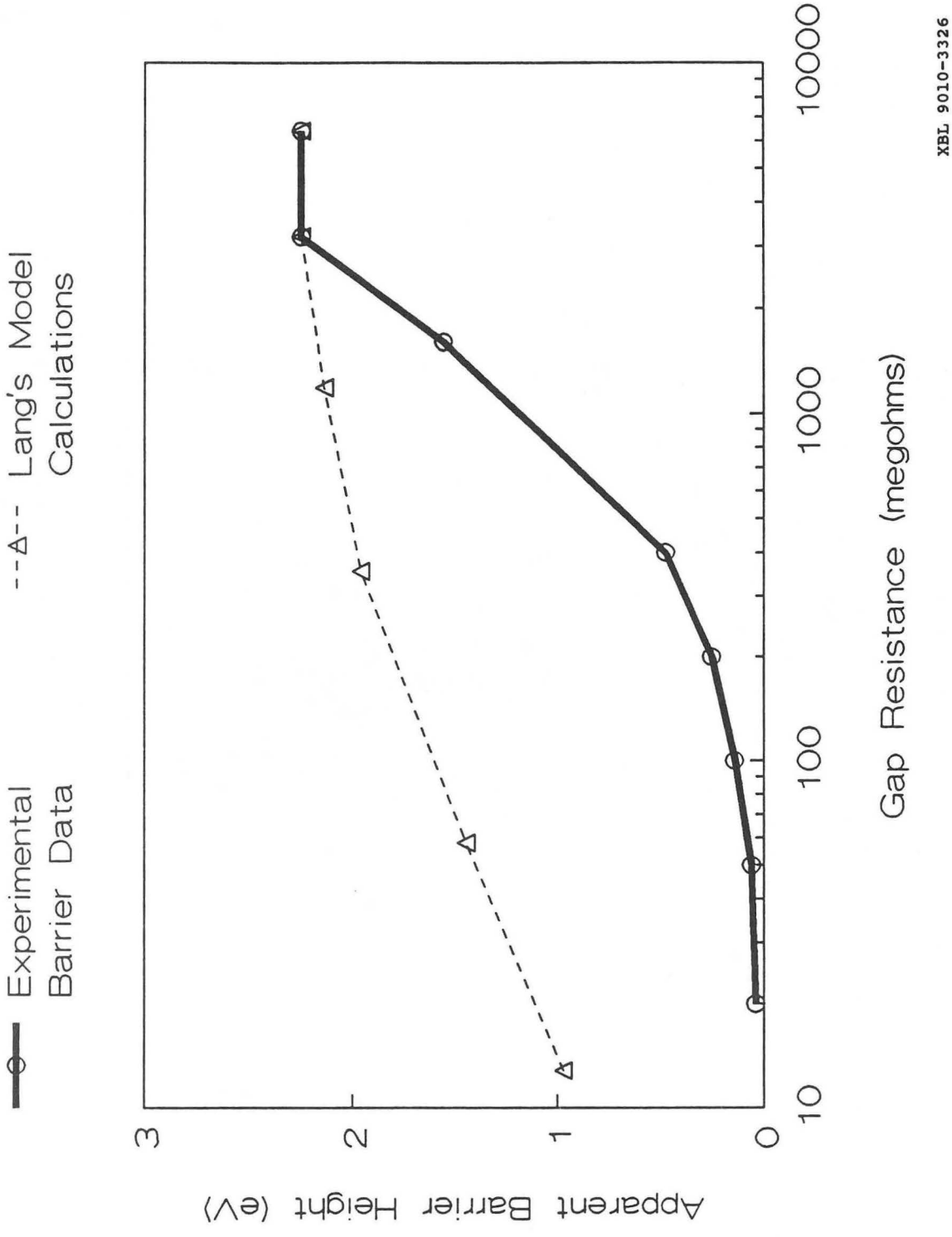
Experimental
Barrier Data
Lang's Model
Calculations
Apparent Barrier Height (eV)
0
1
2
3
10
100
1000
10000
Gap Resistance (megohms)
XBL 9010-3326

Figure 6

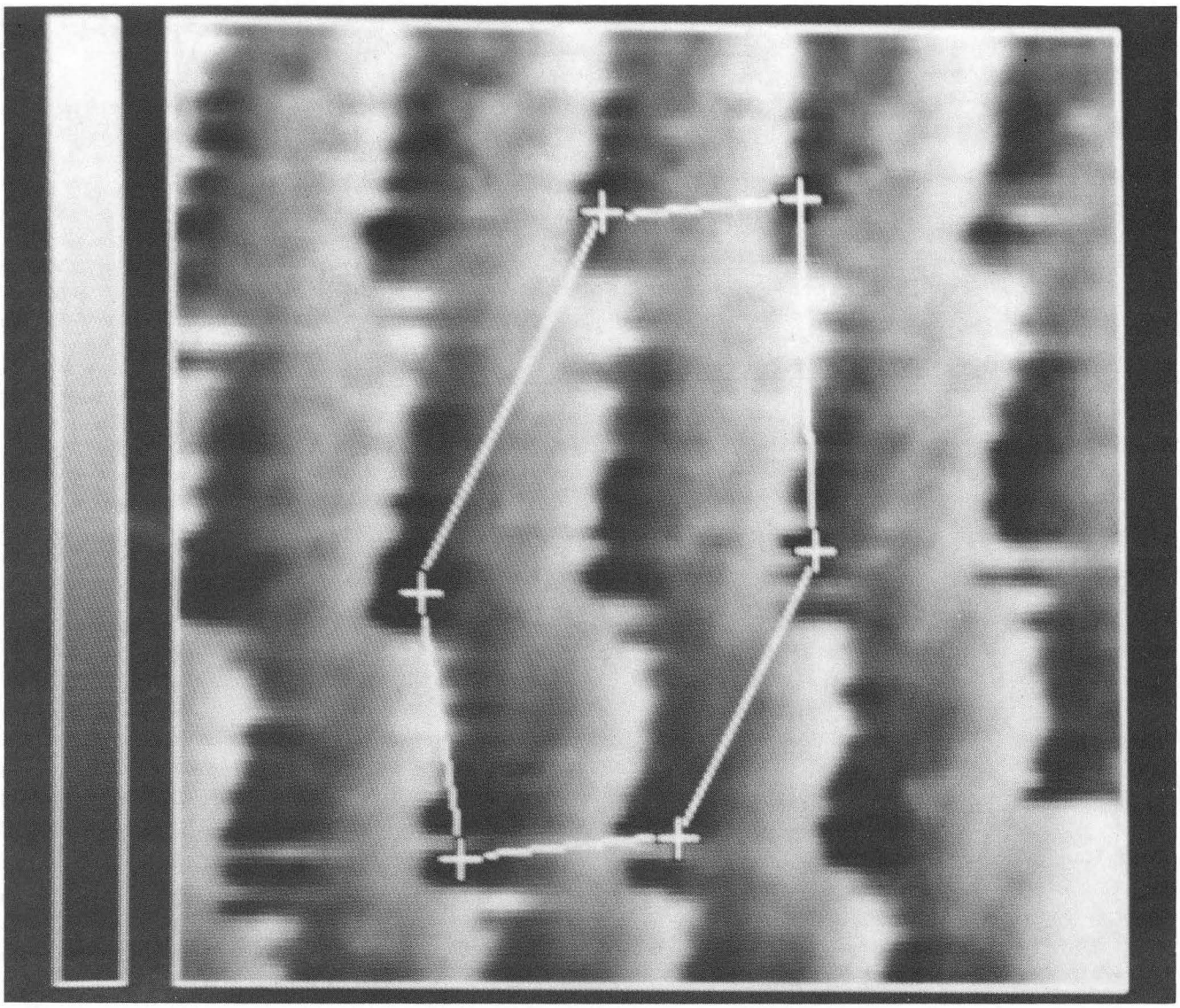

XBB896-5171

Figure 7

LAWRENCE BERKELEY LABORATORY
CENTER FOR ADVANCED MATERIALS
1 CYCLOTRON ROAD
BERKELEY, CALIFORNIA 94720